Acta Geodyn. Geomater., Vol. 19, No. 2 (206), 143–154, 2022
DOI: 10.13168/AGG.2022.0004
journal homepage: https://www.irsm.cas.cz/acta

ORIGINAL PAPER

FINITE ELEMENT BACK ANALYSIS OF GEOSTRESS FIELD IN GEOLOGICAL BODY OF OIL AND GAS TRAP

Meng XU [1], Junwei YANG [2], Shanpo JIA[2],* and Zhenlong CHEN [3]

[1] *School of Earth Sciences, Northeast Petroleum University, Daqing, 163318, China*
[2] *Instiute of Unconventional Oil & Gas, Northeast Petroleum University, Daqing, 163318, China*
[3] *Songyuan Gas Plant, Jilin Oilfield Company, Petro China, Songyuan, 138000, China*

**Corresponding author's e-mail:* jj_luo0321@126.com

ARTICLE INFO

Article history:
Received 21 December 2021
Accepted 8 March 2022
Available online 29 March 2022

Keywords:
Geostress field
Boundary load
Finite element method
Least square method
Finite element inverse approximation

ABSTRACT

The boundary conditions and loading ways of geostress field of oil and gas trap are the difficulties in the numerical simulation and geomechanical analysis. Owing to the limited data of geostress, unclear tectonic movement and complex geological structure, the stress field cannot be solved directly. Boundary load inversion is a very important method to analyze the stress field of rock mass. Based on the measured in-situ stress of S4 member in C41 fault block of Liangjialou oilfield, the boundary loads of the geological body stress field are inversely calculated. Meanwhile, the optimal boundary stress obtained by the inverse modeling is used to study the stress field near the fault. This method can overcome the shortcomings of common back analysis, such as boundary load adjustment method and regression method, and improve the calculation accuracy of stress field. The results show that the inversion method is simple, reliable, accurate and fast. The distribution of stress field can well reflect the in homogeneity of the magnitude and direction of the stress field near the fault. Therefore, this method has a certain application value in boundary load inversion, and the initial stress field distribution of faults provides a precondition for local stability.

1. INTRODUCTION

The in-situ stress is the original stress formed by the joint action of geological structure and self-weight in the geological body. The determination of the initial in-situ stress field is the basis of engineering analysis and design, which is very important for the stability and safety of the project (Guo and Hou, 2020; Li and Miao, 2017; Kang et al., 2010). The causes of in-situ stress are very complex. Years of practical measurement and theoretical analysis show that the formation of in-situ stress depends on the stress produced by previous tectonic movement, loading or unloading caused by earth lifting movement, temperature difference stress caused by magmatic activity, and physical and mechanical properties of rock mass caused by underground movement. From the geomechanical point of view, tectonic stress field and gravity stress field are the main components of the present in-situ stress field (Cai, 2013). However, the calculation accuracy of gravity stress and tectonic stress is completely different, and the weight of rock mass can be determined accurately and the variation range is small. According to the terrain conditions, the finite element method used to calculate the gravity stress can meet the engineering requirements in precision, and can be regarded as known value without reverse calculation; the situation of tectonic stress field is different (Hou and Ge, 2007). In oil and gas exploration and development, due to the importance of in-situ stress field, it is urgent to understand the distribution of stress field. However, what people know is the measured data of several well points in a certain area. In order to provide more reliable in-situ stress data for engineering design and construction, it is necessary to carry out inversion calculation and analysis of initial in-situ stress field according to the site geological structure characteristics and the measured data of known well points in the study area, so as to obtain more accurate and widely applicable in-situ stress field (Li et al., 2014; Wollin et al., 2018).

In recent years, in the numerical simulation and analysis of geological body stress field, researchers have done a lot in the state of in-situ stress field, in-situ stress field inversion method and in-situ stress field regression analysis (Martínez-Garzón et al., 2020; Papannastasiou et al., 2017). The knowledge about spatial variation of stress field is an important step in the identification of geodynamic and seismotectonic characteristics. Inversion of focal mechanism solutions is one of the most common methods for determination of stress field and the shape ratio in a tectonic region (Sheikholeslami et al., 2021; Khanban et al., 2021; Pourbeyranvand, 2018). By collecting and counting a large number of measured in-situ stress data in mainland China, the regression analysis of stress field in China are studied, and the basic

Cite this article as: Xu M, Yang J, Jia S, Chen Z: Finite element back analysis of geostress field in geological body of oil and gas trap. Acta Geodyn. Geomater., 19, No. 2 (206), 143–154, 2022. 0**.** DOI: 10.13168/AGG.2022.0004

characteristics of tectonic stress field in China and the surrounding area are summarized (Wang et al., 2012). In addition to large-scale ground stress background research, it is also necessary to analyze and study the in-situ stress distribution law of specific engineering area, because only in this way can we meet the needs of engineering safety and stability analysis (Xu et al., 2021). Using the intelligent optimization algorithm, the in-situ stress field in the study area is inversed, and the calculation results are compared with the measured values (Li et al., 2019; Zhang et al., 2012; Tu et al., 2017). The results show that the calculation accuracy of the improved algorithm is significantly improved. Although these nonlinear inversion methods can be used to analyze the complex regional in-situ stress field, their convergence speed is slow and the parameter selection is too dependent on experience. According to the field measured data, the condition analysis of regional tectonic stress field is carried out, but the boundary load trial and error method or the boundary load adjustment method are mostly used in the numerical analysis, that is, the calculated value is consistent with the field measured value by changing the load continuously, and the theory of inversion is not studied in depth. This method is actually a trial method, which has a large workload and is difficult to find a satisfactory result (Pham et al., 2020; Liu et al., 2020).

In view of this, a boundary load identification method is proposed in this paper. The measured stress data are directly used as parameters, and the damping least square method is used to approximate the load value. Taking the C41 fault block project in Liangjialou oilfield in the southwest of Dongying sag as an example, the back analysis model of in-situ stress field is established, and the effectiveness and practicability of the method are verified by comparing with the measured in-situ stress.

2. STRESS FIELD MODEL OF PETROLEUM TRAP GEOLOGICAL BODY

According to the basic equations and assumptions of elasticity, for any deformed body V with boundary S, the general equation of boundary value problem in elasticity is (Liu et al., 2020):

$$\left.\begin{aligned} &\varepsilon = BU_n \\ &B^T\sigma + Q = 0 \qquad (In\ V) \\ &B_1^T\sigma = P \qquad (On\ the\ S) \\ &\sigma = D\varepsilon \\ &U_n = U_0 \qquad (x,y,z) \in S \end{aligned}\right\} \tag{1}$$

where B is the differential operator matrix; B_1 is the operator matrix; σ is the stress matrix; ε is the strain matrix; Q is the physical matrix; D is the elastic matrix, which depends on the elastic modulus E and Poisson's ratio μ of the formation. Where the operator matrices B and B_1 are:

$$B = \begin{bmatrix} \frac{\partial}{\partial x} & 0 & 0 & \frac{\partial}{\partial y} & 0 & \frac{\partial}{\partial z} \\ 0 & \frac{\partial}{\partial y} & 0 & \frac{\partial}{\partial x} & \frac{\partial}{\partial z} & 0 \\ 0 & 0 & \frac{\partial}{\partial z} & 0 & \frac{\partial}{\partial y} & \frac{\partial}{\partial x} \end{bmatrix},$$

$$B_1 = \begin{bmatrix} l & 0 & 0 & m & 0 & n \\ 0 & m & 0 & l & n & 0 \\ 0 & 0 & n & 0 & m & l \end{bmatrix} \tag{2}$$

where l, m and n are the cosine of the outer normal direction of boundary S.

The study of in-situ stress field is based on the basic equation (1). For example, the formation of geological structure, the stress field caused by fault movement and the change of in-situ stress caused by oilfield injection and production. Equation (1) can be regarded as a positive problem of differential equation for solving "result" with known "cause", that is, to solve the stress field in deformation body with known load. However, in the exploration and development of oil and gas, the problem to be discussed is how to solve the above boundary value problem according to the measured data, which forms the boundary value problem that the "cause" can be deduced from the known "result". Because the problem discussed is expressed in the form of differential equation, this kind of inverse problem is called differential equation inverse analysis in mathematics. Because it is difficult to solve the inverse problem of differential equation, it is usually impossible to obtain its analytical solution. Therefore, numerical calculation method must be used. Almost all numerical methods use the control equation of continuous variables into algebraic equations with finite discrete variables. There are three common numerical methods: difference method, finite element method and boundary element method. Among these three methods, the finite element method is a more effective method, and the applicability of this method is the strongest.

Let the space domain with fault and boundary S be V, and the finite element equation of three-dimensional boundary value problem is:

$$KU_n = F(X) \tag{3}$$

where K is the overall stiffness matrix; U_n is the node displacement matrix; $F(X)$ is the boundary load array; X is the parameter vector describing the unknown boundary load on the study area.

K and $F(X)$ can be further expressed as:

$$K = \sum_{e=1}^{E} K^e, F(X) = \sum_{e=1}^{E} F^e \tag{4}$$

where E is the total number of elements, K^e and F^e are element stiffness matrix and element load array respectively.

Since the oil field obtains stress data rather than displacement, it is necessary to transform (3) into:

$$U_n = K^{-1}F(X) \tag{5}$$

Using the physical equation (stress-strain relationship), the following formula can be obtained:

$$\sigma = DBU_n \tag{6}$$

By substituting equation (5) into equation (6), the following formula can be obtained:

$$\sigma = DBK^{-1}F(X) \tag{7}$$

According to (7), the relationship between joint stress and boundary load can be obtained as follows:

$$\sigma = TF(X) \tag{8}$$

Let $T = DBK^{-1}$, where T is the theoretical transfer matrix between the node stress matrix and the boundary load array. For linear elastic body, T can be considered as determined after the finite element structure model of stratum is determined.

The finite element method is used to transform the boundary value problem into a set of equations expressed by the node stress of the system. Given the mechanical parameters and boundary conditions of the medium, the stress field of the joint can be solved, which is the positive problem of differential equation (boundary value problem). In equation (8), given the node stress or its function value (such as the direction of the principal stress, etc.) and the mechanical parameters of the medium, what needs to be solved is the boundary condition, which is a set of differential equations, and after discretization, it turns out to be a set of algebra equations. Mathematically speaking, it is an inverse problem for solving differential equations. Because the boundary load is unknown, $F(X)$ is unknown. In the block to be studied, only part of the logging stress value is known, so only part of σ is known. In general, it is impossible to calculate the boundary load parameter vector X by equation (8).

3. INVERSION MODEL

Stress field inversion is a data fitting problem. Its essence is to find the optimal model or parameter which can best fit the measured data under certain criteria. The inversion solution is closely related to the best criterion to measure the degree of data fitting, and it is the optimal solution under the optimal criterion. Sometimes, the research area or block has been studied and understood by relevant disciplines, that is, the model (parameters) has certain prior information. The prior information can be used to constrain the optimization criteria or parameters. The measured data of tectonic stress field are usually the stress measured by local well pressure, borehole burst or core stress test, so inversion is called stress inversion. If the least square method is used as the optimization criterion, the stress inversion criterion (or objective function) can be expressed as the following three models (Tang and Qin, 2004).

(1) Constraint model: If σ_L is the observed stress vector of the known research area and σ_C is the calculated stress vector at the observation point, the model can be expressed as follows:

$$\begin{aligned} &\min \Phi(X) = (\sigma_C - \sigma_L)^T(\sigma_C - \sigma_L) \\ &s.t.\ h_1 \le \varphi(X) \le h_2 \\ &a_i \le X_i \le b_i \end{aligned} \tag{9}$$

where σ_C is calculated by finite element method, $\sigma_C = \{\sigma_{C1}, \sigma_{C2}, \cdots, \sigma_{Cm}\}$; σ_L is the measured stress vector, $\sigma_L = \{\sigma_{L1}, \sigma_{L2}, \cdots, \sigma_{Lm}\}$; m is the number of observation points; $\varphi(X)$ is the constraint function of the boundary load parameter; h_1 and h_2 are the upper and lower bounds of the boundary load parameter function determined according to prior knowledge; X is the boundary load vector to be solved; a_i and b_i are the upper and lower bounds of the boundary load parameters determined according to prior knowledge.

(2) Unconstrained model: When the condition in equation (9) does not exist, it is an unconstrained model:

$$\min \Phi(X) = \left\| \sigma_C - \sigma_L \right\| \tag{10}$$

where σ represents stress tensor, which includes both magnitudes and directions. $\| \cdot \|$ represent norm.

(3) Joint model: If the stress value of the study area and the measured data of the principal stress direction are known, the sum of the residual squares of the stress magnitude and angle is:

$$\min \Phi(X) = \sum (1-\gamma)\frac{\left\| \sigma_L - \sigma_C \right\|}{\sigma_L} + \gamma \frac{\left\| \theta_L - \theta_C \right\|}{\theta_L} \tag{11}$$

where θ_L and θ_C are the measured and finite element values of the principal stress direction at the observation point respectively; γ is the relative weight, which generally takes a value from 0 to 1.The joint model inversion model can be divided into constrained model and unconstrained model. In addition, the eq. (11) is singular for σ_L=0 or θ_L=0.

4. OPTIMIZED INVERSION ALGORITHM

The optimization calculation is related to the finite element simulation. In order to facilitate the application of optimization method in finite element simulation, Sequential Unconstrained Minimization Technique (SUMT) is used to derive the optimization numerical calculation model associated with finite element calculation (Tang and Qin, 2004). The main idea of the model is to transform the constrained problem into unconstrained problem by adding penalty function.

Consider constrained optimization problems:

$$\begin{cases} \min & f = f(x) \\ s.t. & g_i(x) \le \bar{g}_i, \quad i = 1,2,3,\cdots,m_1 \\ & \underline{h}_i \le h_i(x), \quad i = 1,2,3,\cdots,m_2 \\ & \underline{w}_i \le w_i(x) \le \bar{w}_i, \quad i = 1,2,3,\cdots,m_3 \\ & x \in X \subset R^n, \quad x = (x_1, x_2, x_3, \cdots, x_n)^T \end{cases} \tag{12}$$

where f, is the objective function; x is the design variable; g_i, h_i, w_i are the state variables, which can be expressed as the function of the main stress direction and stress, $\underline{h}_i$ and $\underline{w}_i$ are the upper limit values, $\bar{g}_i$ and $\bar{w}_i$ are the lower limit values; $m = m_1 + m_2 + m_3$ is the total number of state variables. State variable changes with design variable x and are called dependent variable.

The unconstrained deduction of constrained problem (12) is carried out. The unconstrained objective function is as follows:

$$Q(x,q) = \frac{f}{f_0} + \sum_{i=1}^{n} P_x(x_i) + \\ + q\left(\sum_{i=1}^{m_1} P_g(g_i) + \sum_{i=1}^{m_2} P_h(h_i) + \sum_{i=1}^{m_3} P_w(w_i) \right) \tag{13}$$

where Q is the dimensionless unconstrained objective function; P_x and P_g, P_h, P_w are the penalty terms of constrained design variables and state variables respectively; f_0 is the reference objective function value introduced for unified unit; q is the penalty factor.

When designing the search direction, if function Q is written as the sum of two functions, a reliable computing advantage can be obtained:

$$Q(x,q) = Q_f(x) + Q_p(x,q) \tag{14}$$

Functions Q_f and Q_p involve objective function and penalty constraint respectively:

$$Q_f(x) = \frac{f}{f_0} Q_p(x,q) = \\ = \sum_{i=1}^{n} P_x(x_i) + q\left(\sum_{i=1}^{m_1} P_g(g_i) + \sum_{i=1}^{m_2} P_h(h_i) + \sum_{i=1}^{m_3} P_w(w_i) \right) Q_p(x,q) = \\ = \sum P_x \frac{f}{f_0}$$

The iterative formula of design variable optimization for unconstrained objective function Q is as follows:

$$x^{(j+1)} = x^{(j)} + S_j d^{(j)} \tag{15}$$

Adjust $x^{(j)}$ and the line search parameter S_j to find the minimum value of Q in direction $d^{(j)}$. Using the golden section method and quadratic interpolation method to solve S_j, the upper and lower limits of S_j are as follows:

$$0 \le S_j \le \frac{S_{\max}}{100} S_j^* \tag{16}$$

where S_j^* is a large number of possible steps in current iterative line search and $S_{\max}$ is the maximum step size of line search.

The key to the solution is the global minimum of the objective function $Q(x,q)$, which depends on the search direction and the internal adjustment of penalty factor q. For the initial iteration $(j = 0)$, the search direction is assumed to be the negative gradient of unconstrained objective function:

$$d^{(0)} = -\nabla Q(x^{(0)}, q) = d_f^{(0)} + d_p^{(0)} \tag{17}$$

If $q = 1$, then

$$d_f^{(0)} = -\nabla Q_f(x^{(0)}), d_p^{(0)} = -\nabla Q_p(x^{(0)}) \tag{18}$$

Obviously, the initial iterative search method is the steepest descent. For the later iteration ($j > 0$), the search direction is formed according to the following recursive formula:

$$d^{(j)} = -\nabla Q(x^{(j)}, q) + r_{j-1} d^{(j-1)} \tag{19}$$

$$r_{j-1} = \frac{\left[\nabla Q(x^{(j)},q) - \nabla Q(x^{(j-1)},q)\right]^T \nabla Q(x^{(j)},q)}{\left|\nabla Q(x^{(j-1)},q)\right|^2} \tag{20}$$

The optimization method ends at convergence or termination. The previous design sequence $(j-1)$ is compared with the current design sequence $(j = 0)$, the problem converges when the following conditions are satisfied:

The change value of the objective function from the current design to the previous design is less than the objective function tolerance:

$$\left| f^{(j)} - f^{(j-1)} \right| \le \tau \tag{21}$$

where τ is the objective function tolerance.

If the following formula occurs, the iteration is terminated and the problem is interrupted before convergence:

$$n_i = N_i \tag{22}$$

where n_i is the iteration algebra and N_i is the allowable number of iterations.

The specific method of finite element inversion of stress field is as follows: select a reasonable objective function, adjust and search parameters by using optimization method, use finite element numerical algorithm to forward calculate value, replace measured value and calculated value into objective function, judge the size of objective function, if the objective function does not reach minimum, continue to adjust and search parameters with optimization method, repeat the above process when the objective function reaches the minimum value, the boundary load parameters can be obtained,

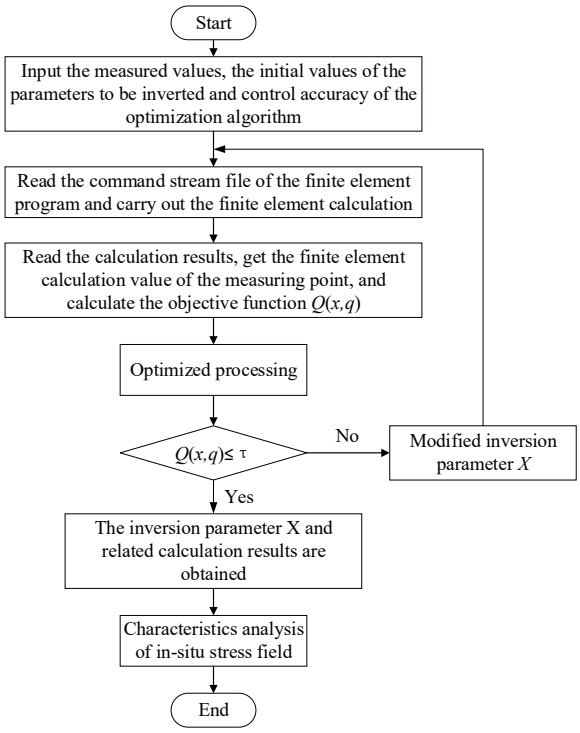

Fig. 1 Finite element inversion process

and the structural stress field can be obtained by using the inverse boundary load for forward calculation. The finite element inversion process is shown in Figure 1.

5. EXAMPLE AND ENGINEERING APPLICATION

With the help of the finite element numerical simulation technology and ANSYS software, the finite element model of the C41 fault block in the southwest of Dongying depression is established, and the finite element iterative program for reverse calculation of the boundary force of the tectonic stress field is compiled. The application of the reverse technology of the boundary load of the tectonic stress field in petroleum geology is studied, and the simulation results of the present in-situ stress field of the C41 fault block are also studied.

5.1. PROJECT OVERVIEW

C41 fault block is a NE trending fault block sandwiched by two NNW trending faults, adjacent to Niuzhuang Sag in the East, Lijin sag in the northwest, and Chunbei fault in the south, adjacent to Chunhua oilfield. The fault block is high in the southwest and low in the northeast. The main reservoir is of the S4, which is mainly composed of fine sandstone. The changes of stratum dip and dip angle are obvious. The structure location map of the top surface of S4 member in C41 fault block is shown in Figure 2.

5.2. PROJECT OVERVIEW

The geological model is the prerequisite for the numerical simulation of in-situ stress field. The determination of the geological model is the basis of

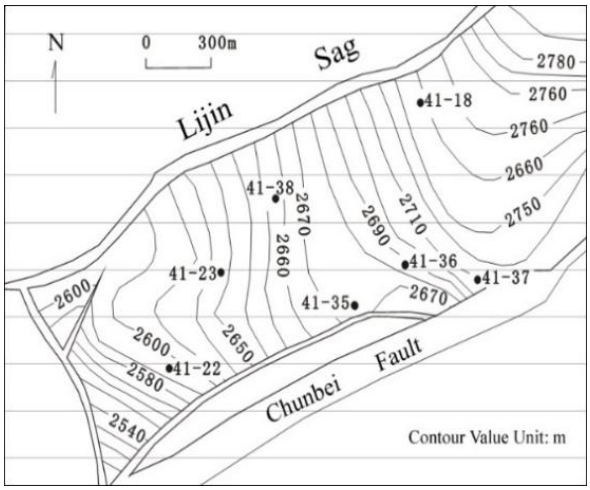

Fig. 2 Structure location map of the top surface of S4 member in C41 block.

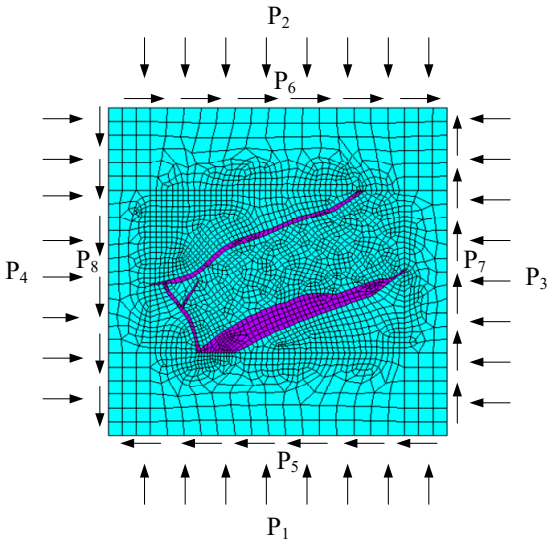

Fig. 3 Study regional mechanical model.

the numerical simulation. The target layer is regarded as the isolation body of a rock block as the object of calculation and simulation. In addition, the geological data of local well points on the target layer, including core data, logging data and oil well dynamic data, should be collected to establish the macroscopic geological model of simulation calculated. In addition, in order to eliminate the influence of boundary conditions, the study area should be expanded on the basis of geological isolation body. In general, the determination of the calculation area should follow the following two principles: (1) The geometric range should be appropriately increased to reduce the influence of boundary conditions on the study area; (2) The geometric constraints at the boundary can be easily determined. The mechanical model of the study area is shown in Figure 3, which is a square calculation area with a side length of 5.5km. Four fault zones are considered in the model. Because the underground sedimentary rock mass is mostly layered, the plane

Table 1 Physical and mechanical parameters of rock in C41 fault block geological mode (Liu et al., 2003).

Horizon	Elastic modulus (MPa)	Poisson's ratio	Density (g/cm^3)
Fault block domain	48000	0.21	2.42
Fault zone	28800	0.28	2.25
Border field	48000	0.21	2.42

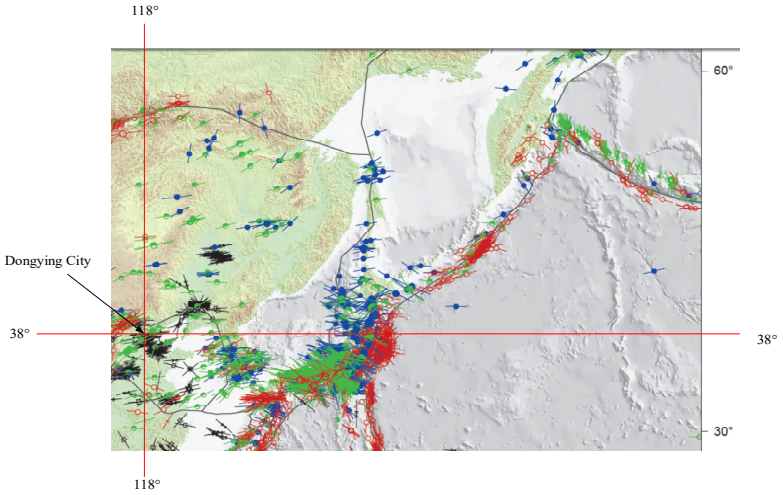

Fig. 4 The location map of Dongying City in the world geostress map.

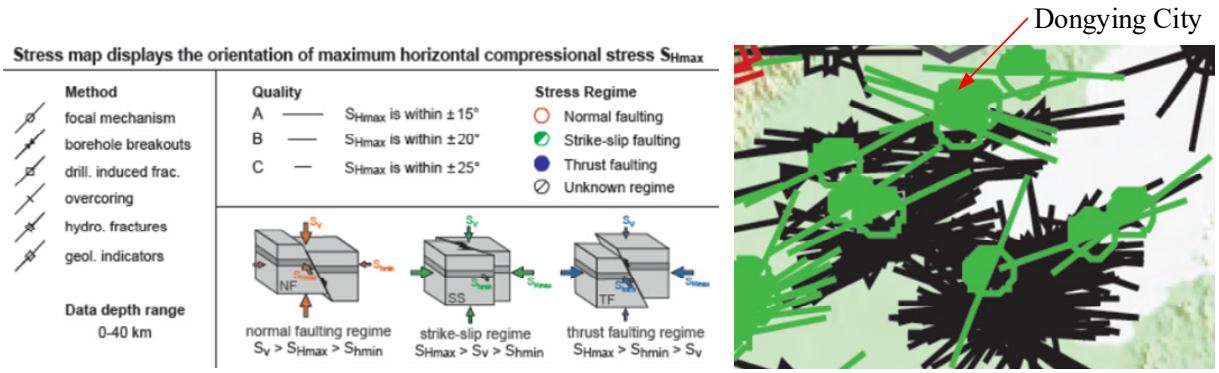

Fig. 5 Local enlarged drawing and icon meaning of Dongying City.

problem of elasticity can be considered in the comprehensive mathematical model (Song et al., 2018; Yan et al., 2018).

The model is divided into 3489 elements and 3496 nodes by using quadrilateral elements. The edge length of the selected elements in the fault zone and its vicinity is relatively small, the mesh is relatively dense, and the mesh of other parts is relatively large. At the same time, the "density" technology is used in the area where "small angle unit" may appear. The model basically reflects the structural characteristics of the main structure, and simplifies the strata and faults. The schematic diagram of finite element mesh model of geological isolation body is shown in Figure 3.

5.3. ROCK MECHANICS PARAMETERS AND IN-SITU STRESS OF MEASURING POINTS

At present, the determination of rock physical parameters of different layers and different structural parts of geological bodies is generally based on the macro effect, and the geological body is approximately regarded as a block of uniform rock body. The fault is treated as a fault zone, the strength of the filling lithology within a proper distance on both sides of the fault will be weakened, and the Young's modulus and other mechanical parameters of the rock will be reduced by a certain proportion compared with the lithology with the same depth. This is the principle often adopted in stress field simulation (Tian et al., 2021). The petrophysical parameters of the geological model of C41 fault block in the study area are shown in Table 1.

Since the C41 fault block in the study area is located in Dongying City, Shandong Province, and its geographical location is 118 ° E and 38 ° N, its approximate position in the world geostress map (Heidbach et al., 2016) is shown in Figure 4, and the local enlarged map and icon meaning of Dongying City are shown in Figure 5.

Table 2 Measured stress components of measurement points under computation coordinate systém.

Measuring point	Stress component	Measured value (MPa)
41-18	σ_x	-65.969
	σ_y	-52.231
	τ_{xy}	-5.816
41-22	σ_x	-64.055
	σ_y	-52.545
	τ_{xy}	-6.919
41-23	σ_x	-64.585
	σ_y	-51.515
	τ_{xy}	-6.826
41-35	σ_x	-68.33
	σ_y	-55.27
	τ_{xy}	-4.846
41-36	σ_x	-66.296
	σ_y	-52.304
	τ_{xy}	-4.081
41-37	σ_x	-64.393
	σ_y	-53.606
	τ_{xy}	-5.634
41-38	σ_x	-65.968
	σ_y	-54.031
	τ_{xy}	-4.905

Figure 5 shows the direction of the maximum horizontal stress S_{Hmax} in Dongying City is approximately within 20 ° East by South. The rock mass of the two walls along the strike of the fault plane is horizontal relative movement, and it is a translation fault. The stress field size state is $S_{Hmax}>S_v>S_{hmin}$.

In the analysis of in-situ stress field, the basic object is to calculate the coordinate stress component in the coordinate system XY, but the measured value of in-situ stress is generally given according to the azimuth and dip angle of the principal stress. The direction cosine between the measured principal stress and the coordinate axis should be calculated first:

$$\begin{cases} l_i = \cos\alpha_i \\ m_i = \cos\left(\dfrac{\pi}{2} - \alpha_i\right) \end{cases} \tag{23}$$

Where l is the direction cosine between stress and x axis; m is the direction cosine between stress and y axis; α is the angle between stress and x.

According to the field test data (Dai and Li, 2011), the principal stress is converted into the stress component in the calculation coordinate system by the following formula:

$$\begin{cases} \sigma_x = l_1^2\sigma_1 + l_3^2\sigma_3 \\ \sigma_y = m_1^2\sigma_1 + m_3^2\sigma_3 \\ \tau_{xy} = l_1m_1\sigma_1 + l_3m_3\sigma_3 \end{cases} \tag{24}$$

where σ_1 is the maximum principal stress and σ_3 is the minimum principal stress.

After conversion, the measured stress components of 7 measuring points are obtained, as shown in Table 2.

5.4. BOUNDARY INVERSION OF TECTONIC STRESS FIELD OF S4

One of the most difficult and important problems in the simulation of tectonic stress field with finite element method is to determine the boundary conditions of the block, especially the far-field stress (horizontal boundary stress) is the key to determine the stress properties in the field. Generally, the calculation block should be large enough and the surrounding strata should be relatively flat. Because the stress field of oil and gas reservoir is the focus of research, the vertical variation of tectonic stress can be ignored when the total thickness of reservoir is less than 200 m, and the horizontal boundary force basically does not change with the burial depth. Therefore, the horizontal boundary stress (far-field stress) can be inversed by using the plane stress model of reservoir. Optimization inversion is mainly used in two-dimensional model to speed up the calculation and save calculation time.

(1) Initial condition of model boundary: Two edge points on the east boundary of the model are fixed to ensure that there is no rigid body translation and rotation in the study area; The South, North, East and West boundaries of the model are subjected to uniform compressive stress, which are denoted as P_1, P_2, P_3 and P_4. The initial values of boundary forces are 50 MPa, 50 MPa, 65 MPa and 65 MPa respectively; The South, North, East and West boundaries of the model are subjected to uniformly distributed shear stress, which are denoted as P_5, P_6, P_7 and P_8. The initial values of boundary forces are 5 MPa, 5 MPa, 10 MPa and 10 MPa. The action mode of boundary force is shown in Figure 3.

(2) Inversion parameter selection: The 21 stress components of 7 measuring points were used as measured values to invert the 8 unknown boundary forces in the study area. The distribution of measuring points is shown in Figure 2, and the measured values of 21stress components are shown in Table 2.

(3) Calculation conditions: The sum of squares of the stress residuals between the calculated values and the measured values is used as the objective function. The lower limit and upper limit of boundary compressive stress constraint value are 10 MPa and 100 MPa respectively; The lower limit and upper limit of boundary shear stress constraint value are -25 MPa and 25 MPa respectively, the iteration termination accuracy is 10^{-5} MPa^2. At the same time, boundary force constraint should be considered to make the resultant force and resultant moment of boundary force zero.

(4) Inversion results: Based on the above conditions, the calculated values of measured points are shown in Figure 6; the variation curves of stress components of some measuring points 41-18, 41-22 and 41-23 with iteration algebra are shown in Figure 7, Figure 8 and Figure 9 respectively.

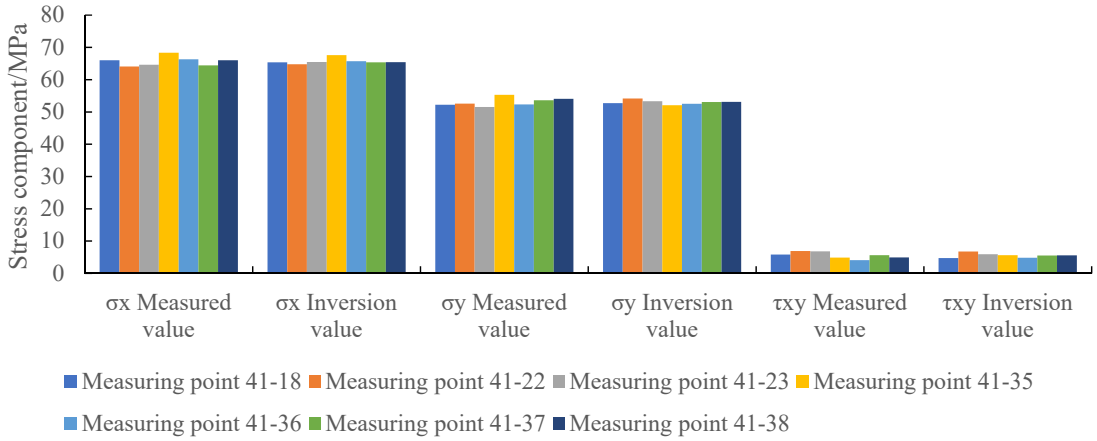

Fig. 6 Comparison of inversion value and measured value.

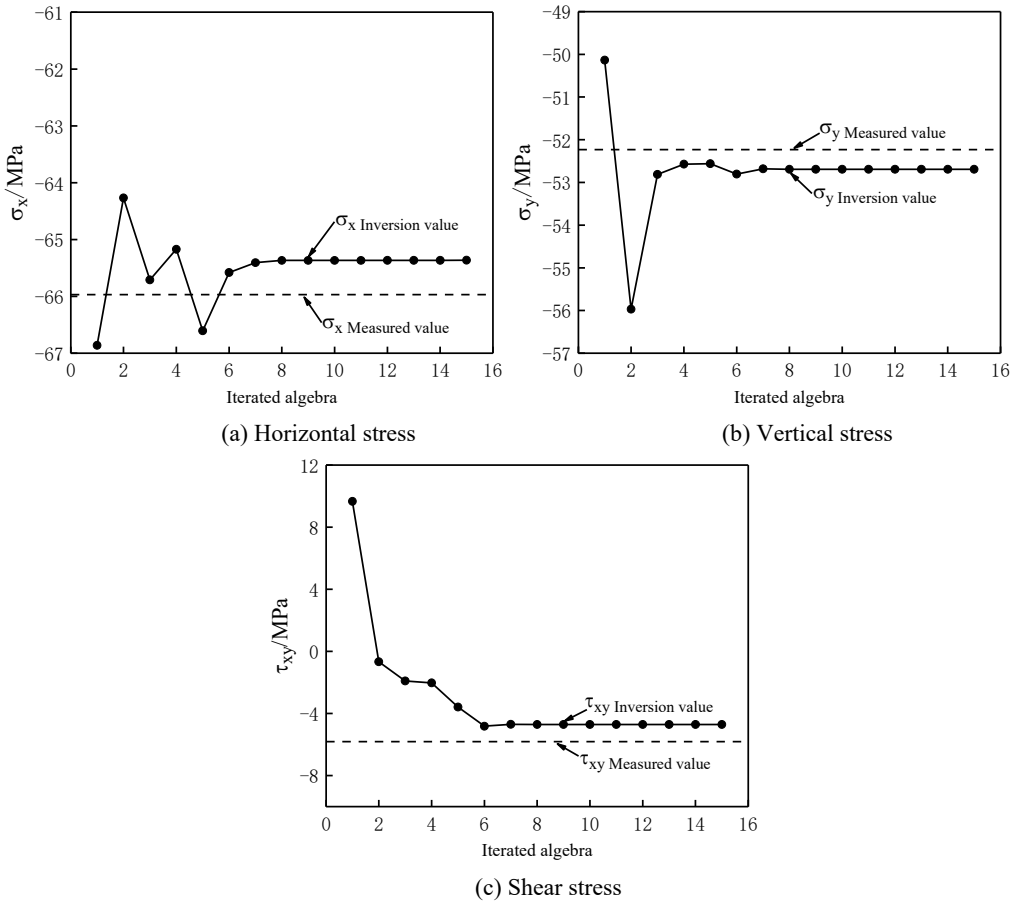

Fig. 7 Stress variation diagram of 41-18 measuring points with iteration.

It can be seen from Figure 6 that the relative error of stress components σ_x and σ_y is basically controlled within 3 % (except the vertical stress component of well point 41-35); The relative error of shear stress component is controlled within 20 %. The stress values of each well point have reached or very close to the test values, the relative error is basically controlled within 10 %, and the accuracy of inversion results basically meets the requirements of engineering practice. The optimal value of horizontal tectonic boundary force is shown in Table 3.

5.5. ANALYSIS OF IN-SITU STRESS FIELD OF S4

The optimal boundary force obtained from optimization inversion is applied to the boundary of the calculation model, and the in-situ stress distribution of the target layer can be obtained by forward calculation. The maximum horizontal principal compressive stress size and direction superposition diagram, and the minimum principal compressive stress size and direction superposition diagram are shown in Figure 10 and Figure 11 respectively.

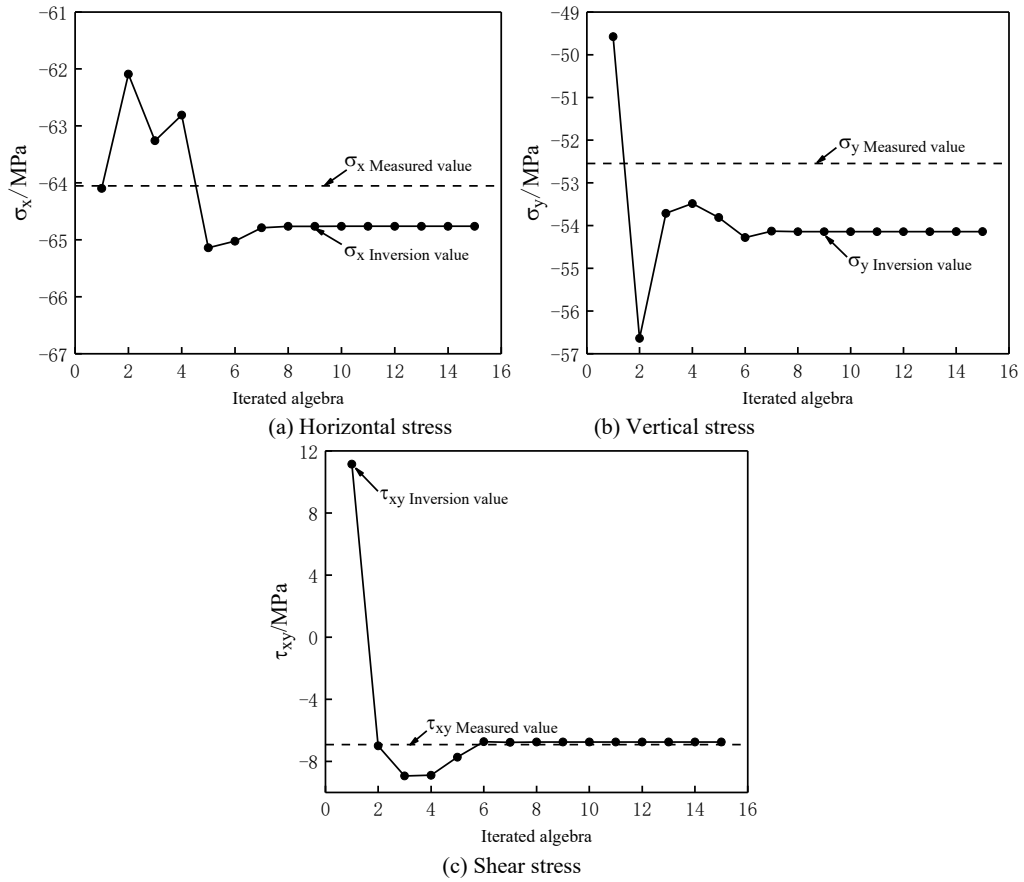

Fig. 8 Stress variation diagram of 41-22 measuring points with iteration.

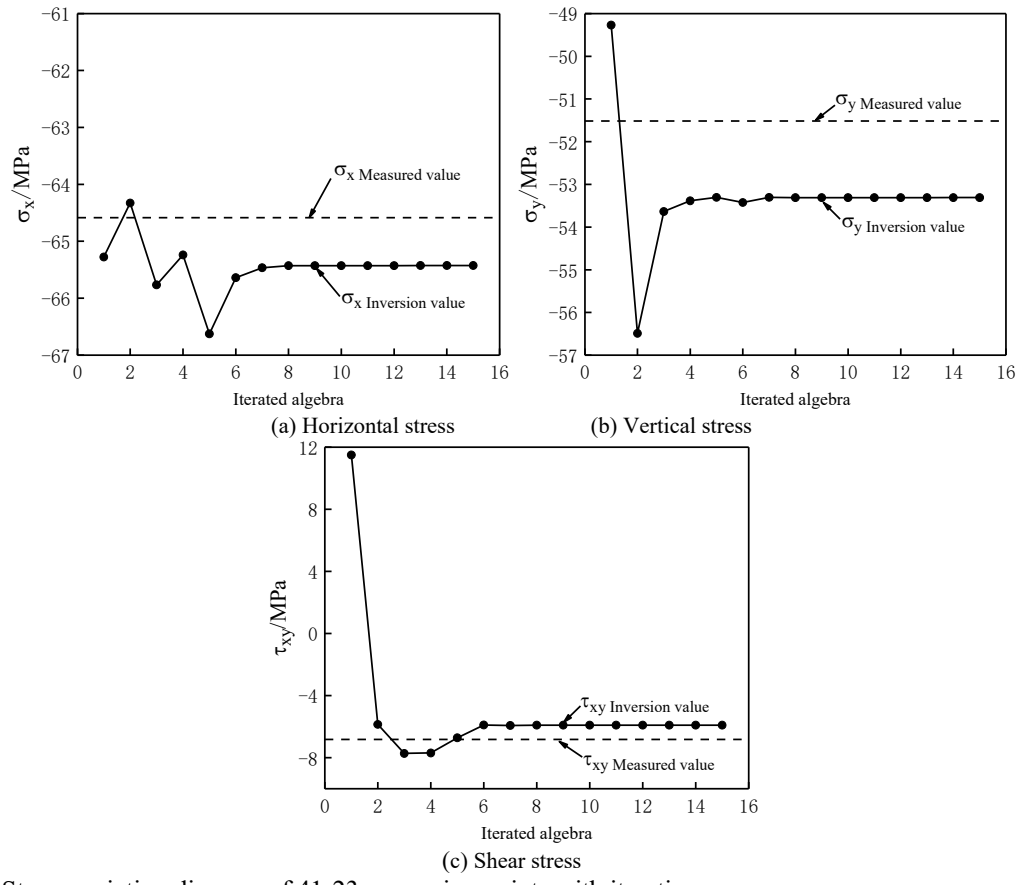

Fig. 9 Stress variation diagram of 41-23 measuring points with iteration.

Table 3 The optimum results of boundary loads (unit: MPa).

P_1	P_2	P_3	P_4	P_5	P_6	P_7	P_8
53.645	53.645	64.466	64.466	-5.96	-5.96	-5.099	-5.099

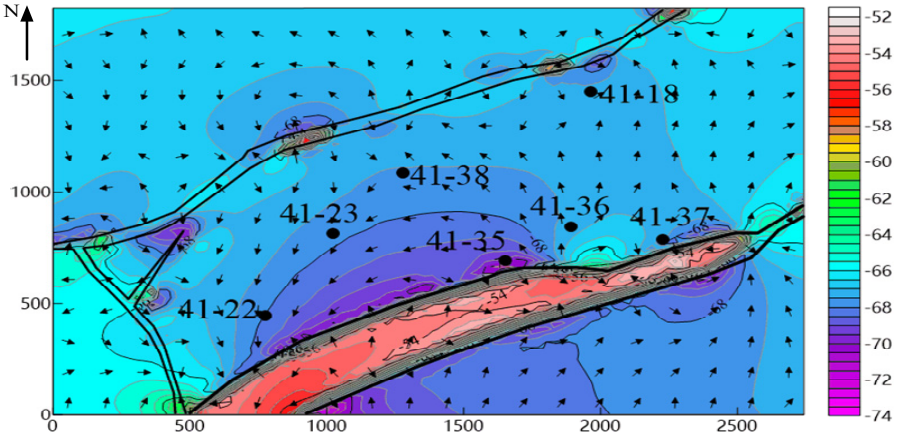

Fig. 10 Superposed diagram of magnitude and direction of current horizontal maximum principal compressive stress (unit: MPa).

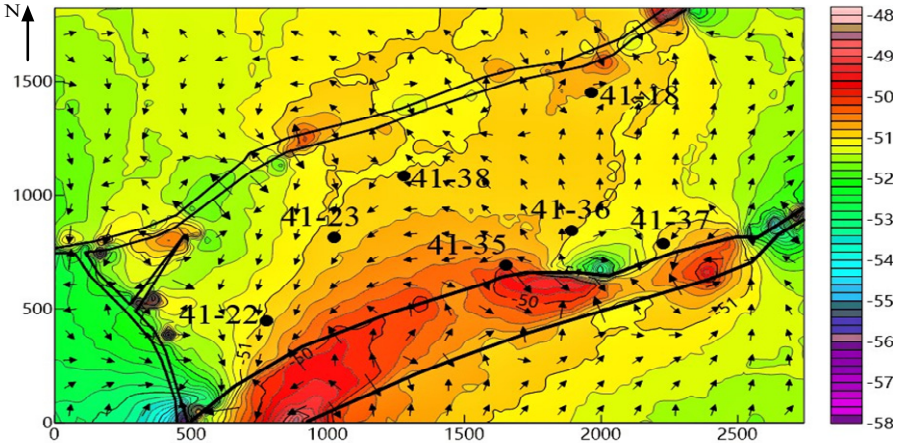

Fig. 11 Superposed diagram of magnitude and direction of current horizontal maximum principal compressive stress (unit: MPa).

It can be seen from Figure 10 and Figure 11 that the maximum horizontal principal compressive stress is between -52 MPa and -74 MPa, and the minimum horizontal principal compressive stress is between - 48 MPa and -58 MPa. Due to the weak mechanical parameters of the fault, obvious stress release phenomenon occurred inside the fault. In the southern boundary fault, the maximum principal stress of rock mass decreased about 10 MPa, and the minimum principal stress decreased about 2 MPa. Due to the compression, the local stress value of the fault edge increased. The gradient zone of principal stress changes is formed near the fault zone, the most obvious in the south boundary fault zone and the second in the northern boundary fault layer. It can also be seen that the direction of the maximum principal stress and the minimum principal stress change obviously within the fault, indicating that the fault has a great disturbance effect on the local stress field direction of S4 member in C41 fault block.

6. CONCLUSION

(1) Faults have significant influence on the magnitude and direction of local stress field. The value of principal stress at the edge of fault zone slightly increases, and the direction of maximum principal stress deflects parallel to the fault plane; in the fault zone, the value of principal stress weakens, and the direction of maximum principal stress deflects perpendicular to the fault plane.

(2) The inversion of in-situ stress field is similar to the geophysical inverse problem. According to the optimization inversion model and convergence criteria, there is a non-uniqueness problem of the solution. It is necessary to apply a priori constraint to

improve the non-uniqueness of the solution. According to the comparison between the logging data and the measured data, the results are screened out and the unreasonable values are eliminated.

(3) Based on the basic equations of elastic mechanics, a numerical inversion model of in-situ stress is established, and the basic influencing factors of stress field are comprehensively considered by using geomechanical analysis method, and a finite element inversion method for boundary load of geological body stress field is proposed. This method overcomes the shortcomings of general back analysis algorithms such as regression inversion method and boundary adjustment method, and comprehensively considers the influence of faults and complex tectonics. It has high inversion accuracy for measured points and reflects the non-uniform characteristics of stress field near the fault. In addition, the method is also practical, almost free from the geometric characteristics and boundary conditions of the geological model.

(4) Due to the influence of faults, the direction of local stress field in the study area is deflected in different degrees. The inversion results accurately obtain the distribution of initial stress field in the study area containing faults, which provides a prerequisite for fracture prediction, well pattern deployment, drilling design and local stability.

ACKNOWLEDGMENTS

The authors gratefully acknowledge the support of the National Natural Science Foundation of China (Grant No. 42072166), the Natural Science Foundation of Heilongjiang Province (Grant No. LH2020D004) and the State Key Laboratory project of Deep Geotechnical Mechanics and Underground Engineering (Grant No. SKLGDUEK2001).

REFERENCES

Cai, M.F.: 2013, Rock mechanics and Engineering. Science Press, Beijing, 125–134.

Dai, J.S. and Li, L.: 2011, Structural analysis of oil province. China University of Petroleum Press, Dongying, 167–189.

Guo, Y.H. and Hou, K.P.: 2020, Inversion method of initial high level tectonic stress field of rock mass based on flac3D. Science Technology and Engineering, 20, 21, 8523–8529.

Heidbach, O., Rajabi, M., Reiter, K. and Ziegler, M.: 2016, World Stress Map 2016. GFZ Data Service. DOI: 10.5880/WSM.2016.002

Hou, M.X. and Ge, X.R.: 2007, Study on fitting analysis of initial stress field in rock masses. Rock Soil Mech., 28, 8, 1626–1630. DOI: 10.16285/j.rsm.2007.08.027

Kang, H., Zhang, X., Si, L., Wu, Y. and Gao, F.: 2010, In-situ stress measurements and stress distribute characteristics in underground coal mines in China. Eng. Geol., 116, 3-4, 333–345. DOI: 10.1016/j.enggeo.2010. 09.015

Khanban, M.A., Pakzad, M., Mirzaei, N., Moradi, A. and Mehramuz, M.: 2021, The present-day stress field in the Zagros Fold-Thrust Belt of Iran, from inversion of focal mechanisms. J. Geodyn., 143, 101812. DOI: 10.1016/j.jog.2020.101812

Li, P. and Miao, S.J.: 2017, Analysis and application of in-situ stress in metal mining area of Chinese mainland. Chin. J. Eng., 39, 3, 323–334. DOI: 10.13374/j.issn2095-9389.2017.03.002

Li, M.H., Yang, Z.Q., Gao, Q., Zhai, S.H. and Wang, Y.T.: 2014, Research on intelligent identification methods for in-situ stress field base on complex geological body. Rock Soil Mech., 35, s2, 638–644. DOI: 10.16285/j.rsm.2014.s2.026

Li, F., Zhou, J.X. and Wang, J.A.: 2019, Back-analysis and reconstruction method of in-situ stress field based on limited sample data. J. China Coal Soc., 44, 5, 1421–1431. DOI: 10.13225/j.cnki.jccs.2018.6002

Liu, J.S., Yang, H.M., Wu, X.F. and Liu, Y.: 2020, The in situ stress field and microscale controlling factors in the Ordos Basin, central China. Int. J. Rock Mech. Mining Sci., 135, 104482. DOI: 10.1016/ j.ijrmms.2020.104482

Liu, X.T., Dai, J.S., Xu, J.C. and Wang, B.F.: 2003, Finite element simulation of the present ground stress field of Sha-4 member in the Chun-41 fault block. Pet. Explor. Dev., 30, 3, 126–128, (in Chinese). http://www.cpedm.com/CN/Y2003/V30/I3/2.

Martínez-Garzón, P., Heidbach, O. and Bohnhoff, M.: 2020, Contemporary stress and strain field in the Mediterranean from stress inversion of focal mechanisms and GPS data. Tectonophysics, 774, 228286. DOI: 10.1016/j.tecto. 2019.228286

Papanastasiou, P., Kyriacou, A. and Sarris, E.: 2017, Constraining the in-situ stresses in a tectonically active offshore basin in Eastern Mediterranean. J. Pet. Sci. Eng., 149, 208–217. DOI: 10.1016/j. petrol.2016.10.033

Pham, C., Chang, C.D., Jang, Y., Kutty, A. and Jeong, J.: 2020, Effect of faults and rock physical properties on in situ stress within highly heterogeneous carbonate reservoirs. J. Pet. Sci. Eng., 185, 106601. DOI: 10.1016/j.petrol.2019.106601

Pourbeyranvand, S.: 2018, Stress studies in the Central Alborz by inversion of earthquake focal mechanism data. Acta Geophys., 66, 1273–1290. DOI: 10.1007/s11600-018-0207-1

Sheikholeslami, M.R., Mobayen, P., Javadi, H.R. and Ghassemi, M.R.: 2021, Stress field and tectonic regime of Central Iran from inversion of the earthquake focal mechanisms. Tectonophysics, 813, 228931. DOI: 10.1016/j.tecto.2021 228931

Song, Z.F., Sun, Y.J. and Lin, X.: 2018, Research on in situ stress measurement and inversion, and its influence on roadway layout in coal mine with thick coal seam and large mining height. Geotech Geol. Eng., 36, 1907–1917. DOI: 10.1007/s10706-017-0427-1

Tang, H.W. and Qin, X.Z.: 2004, Practical optimization method. Dalian University of Technology Press, Dalian, 155–169.

Tian, H., Zeng, L.B, Xu, X., Li, H., Luo, B. and Dong, S.Q.: 2021, Factors influencing the in-situ stress orientations in shales: A case study of the Wufeng-Longmaxi formations in the Jiaoshiba Area, southeastern Sichuan Basin, China. J. Nat. Gas Sci. Eng., 94, 104110. DOI: 10.1016/j.jngse.2021.104110

Tu, T., Wang, J. and Zhang, M.D.: 2017, Application of BP neural network based improved PSO in initial geostress field inversion optimization. Water Resources and Power, 35, 12, 123–126+139.

Wang, Y.H., Cui, X.F., Hu, X.P. and Xie, F.R.: 2012, Study on the stress state in upper crust of China mainland based on in-situ stress measurements. Chin. J. Geophys., 55, 9, 3016–3027. DOI: 10.6038/j.issn.0001-5733.2012.09.020

Wollin, C., Bohnhoff, M., Vavryčuk, V. and Martínez-Garzón, P.: 2018, Stress inversion of regional seismicity in the Sea of Marmara region, Turkey. Pure Appl. Geophys., 176, 1357. DOI: 10.1007/s00024-018-1971-1

Xu, D.P., Huang, X., Jiang, Q., Li, S.J., Zheng, H., Qiu, S.L., Xu, H.S., Li, Y.H., Li, Z.G. and Ma, X.D.: 2021, Estimation of the three-dimensional in situ stress field around a large deep underground cavern group near a valley. J. Rock Mech. Geotech. Eng., 13, 3, 529–544. DOI: 10.1016/j.jrmge.2020.11.007

Yan, X.L., Zhang, J., Song, S., Li, M.Q., Gao, Y., Hu, T.J. and Ke, H.Q.: 2018, Research on in-situ field in Shouyang block. J. Xi'an Shiyou Univ. Nat. Sci., 33, 2, 16–23. DOI: 10.3969/j.issn.1673-064X.2018.02.003

Zhang, L.W., Zhang, D.Y. and Qiu, D.H.: 2012, Application of radial basis function neural network to geostress field back analysis. Rock Soil Mech., 33, 3, 799–804. DOI: 10.16285/j.rsm.2012.03.038